HIGH-SPEED IMAGING OF THE IMPACT FLASH: OBSERVATIONS OF SOURCE LOCATION AND TRANSIENT CRATER GROWTH. Carolyn M. Ernst[1], Olivier S. Barnouin[1], and Peter H. Schultz[2], [1]Johns Hopkins University Applied Physics Laboratory, Laurel, MD 20723 (carolyn.ernst@jhuapl.edu), [2]Department of Geological Sciences, Brown University, Providence, RI 02912.

Introduction: Experimental impacts into non-volatile, particulate targets produce long-duration impact flashes dominated by hot thermal sources [e.g., 1-3]. These flashes last orders of magnitude longer than those where the radiation sources are atomic and molecular emissions [e.g., 4-6]. High-speed photometry and imaging of the flash can be used to probe the early-time evolution of the emitting source and the transient crater. Understanding what processes control the generation and evolution of the impact flash is ultimately important for quantifying energy partitioning and melt production during impact and for interpreting planetary impact flashes (e.g., lunar flashes).

Experimental setup: Hypervelocity impact experiments were performed using the two-stage light gas gun at the NASA Ames Vertical Gun Range (AVGR). Pyrex projectiles 6.35 mm in diameter impacted pumice powder targets under near-vacuum conditions (< 0.5 Torr) at angles from 90º (vertical) to 15º. Impact velocities ranged from 4.8 to 5.2 km/s. The predominantly silicate compositions of Pyrex and pumice minimize the production of atomic and molecular emissions in the visible wavelength range and enhance the generation of thermal emissions, which are of primary interest for this study.

Two photodiode systems (described in 7) positioned above the target chamber recorded the visible and near-infrared light output every 100 ns for a total of 2 ms. The field of view of each photodiode was large enough to ensure that all radiating sources would remain observable over the recorded time interval. Two high-speed Shimadzu cameras also recorded the impact flash, from positions above and to the side of the impact chamber. These cameras acquired data at 10^6 fps and 500,000 fps, respectively, both with 200 ns exposure times.

Spatially integrated photometry: The time-resolved, spatially integrated photometry recorded by the photodiodes reveals light curves characterized by a rapid rise to a broad intensity peak, followed by a long-lasting decay. The properties of the broad peak are highly dependent on impact angle (Figure 1). The peak intensity increases with a decreasing impact angle (90º to 30º) as the rise time to this maximum decreases. By 30º, not only does the maximum intensity increase considerably, but also the duration of the broad peak is much shorter. This trend breaks down for 15º; at such low angles, the projectile retains much of its initial kinetic energy after impact.

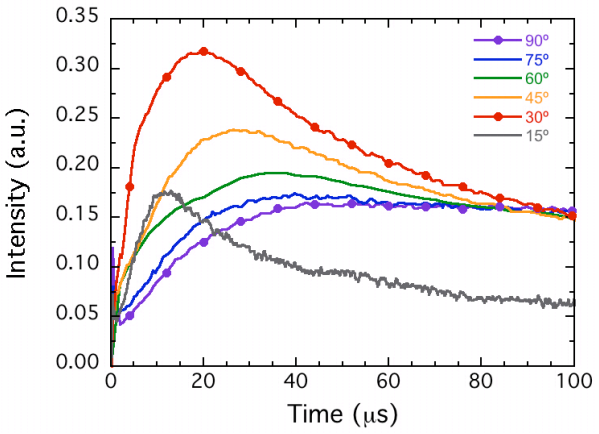

Figure 1. Effect of impact angle on the observed light curves for impacts of 6.35-mm Pyrex projectiles into pumice powder targets between 4.8 and 5.2 km/s. Higher-angle impacts exhibit lower and broader intensity peaks and longer rise times. The maximum peak intensity occurs during the 30º impact. At 15º the projectile is poorly coupled to the target on impact, breaking the observed angular dependence on peak intensity.

The dependences of the light curve characteristics on impact angle relate both to the horizontal (peak intensity) and vertical (rise time) components of the impact velocity, suggesting that the photometric evolution of the impact flash can be related to physical processes.

Spatial resolution and source location: The temperatures of these impact flashes steadily decrease after the moment of impact [7]. Therefore, an increasing source area must control the rise to the broad intensity peak. The analysis of side-view photodiode observations suggests that much of the radiating source is contained within the transient crater [8]. However, the location and distribution of the radiating source cannot be definitively determined by the photodiode measurements alone.

New, high-speed images of the impact flash allow the direct observation of the source area through time, confirm the hypotheses derived from the integrated photometric measurements, and reveal new insights into the evolution of the impact flash. These images (Figure 2) show that for all angles the size of the radiating source increases through time. The integrated brightness at a given time is greatest for a 30º impact (e.g., Figs. 1,2), while the average intensity of an illuminated pixel is greatest for a 90º impact. This means that the radiating source for a 30º impact is larger in area but lower in temperature than for a 90º impact.

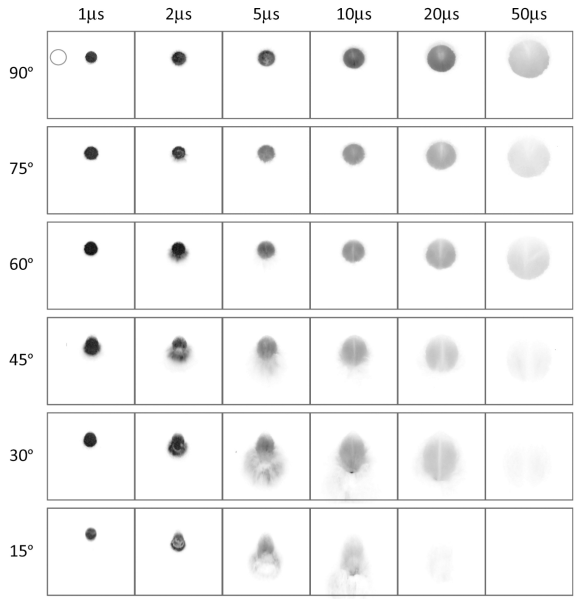

Figure 2. Selected images acquired using the top-view Shimadzu camera. The images have been inverted, and all images were stretched to the same brightness scale. For non-vertical impacts, the direction of impact is from the top of the picture. The unfilled circle represents the size of the projectile for scale. For the more oblique impacts, downrange components of the radiating source can be seen. Although the integrated brightness of a 30º impact is greater than that of a 90º impact, the average intensity of an illuminated pixel (which corresponds to temperature) is greater for the 90º impact.

The differences in source area dominate over the differences in temperature, and the increase in the overall flash brightness with decreasing impact angle is controlled by the increasing exposure of the radiating material within the transient cavity.

As the impact angle decreases from 90º to 30º, a component of radiating material emerges downrange, while the along-trajectory/cross-trajectory aspect ratio of the main radiating source increases. This aspect ratio trend is consistent with expectations for the evolving transient crater: at early stages of crater formation, the transient crater will be narrowest and deepest for a vertical impact; at lower angles the transient crater opening is shallower and elongated parallel to the direction of impact [9].

The position of the radiating source can be constrained further by examining side-view images of the impacts (Figure 3). At 30º, the initial radiating source is located at and just around the penetrating projectile. By 4-6 μs after impact, a downrange component of radiating material emerges. The main radiating source is confined near the point of impact and cannot be observed by the side-view camera, implying that the transient crater walls and the emerging cool ejecta curtain block the radiating material from view. By 8-10 μs after impact, most of the remaining radiating source is located within the evolving transient crater.

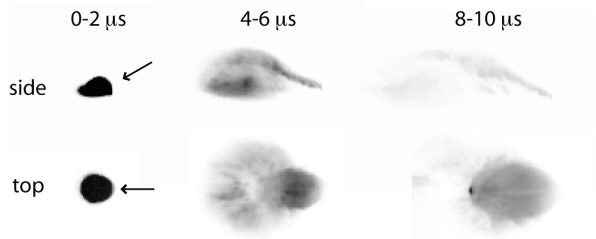

Figure 3. Selected images of the impact flash produced during a 30º impact, acquired from the top- and side-view Shimadzu cameras. Arrows show the direction of impact. The images have been inverted, and each exposure is 200 ns. Just after impact, the radiating material is all located in the area of the projectile. At 4-6 μs after impact, a portion of the radiating material emerges downrange, while the rest remains confined inside of the transient cavity. By 8-10 μs after impact, most of the remaining radiating source is confined within the transient crater, below the pre-impact target surface, and cannot be observed from the side view.

Conclusions: In these experiments, the impact flash results primarily from hot material located within the transient crater cavity. Changes in impact angle affect the geometry of the developing crater during early-time formation, which influences the exposure of the radiating source and the resulting impact flash characteristics. The magnitude and timing of the intensity peak are related to the horizontal or vertical component of velocity, respectively. The rise to the intensity peak is primarily caused by the growth of the radiating source area.

The high-speed images reveal the distribution and evolution of the radiating source, which is located primarily within the transient crater, below the pre-impact surface. At lower impact angles, additional radiating material is visible in the ejecta. Although the integrated intensity is higher for a 30º impact (due to a larger observable source area), the average temperature of the source is higher for a 90º impact, with the intermediate impact angles following this trend. Higher impact angles produce a deeper and more confined radiating source, whereas lower impact angles produce a shallower and more spread out radiating source, resulting in observable differences in impact flash characteristics.

References: [1] Ernst, C. M. and P. H. Schultz (2007) *Icarus*, 190, 334-344. [2] Ernst, C. M. and P. H. Schultz (2002) *LPS* XXXIII, #1782. [3] Ernst, C. M. and P. H. Schultz (2003) *LPS* XXXIV, #2020. [4] MacCormack, R. W. (1963) *Proc. 6th HVIS*, 2, 613- 625. [5] Jean, B. and T. L. Rollins (1970) *AIAA J.*, 8, 1742-1748. [6] Eichhorn, G. (1976) *Planet. Space Sci.,* 24, 771- 781. [7] Ernst, C. M. and P. H. Schultz (2004) *LPS* XXXV, #1721. [8] Ernst, C.M. and P. H. Schultz (2008) *LPS* XXXIX, #1391. [9] Schultz, P. H. et al. (2005) *SSR* 117, 207-239.